

Effect of interlayer bonded bilayer graphene on friction

Yao-Long Li(李耀隆), Zhen-Guo Tian(田振国), Hai-Feng Yin(尹海峰), and Ren-Liang Zhang(张任良)
Citation: Chin. Phys. B, 2024, 33 (**8**): 086103. DOI: 10.1088/1674-1056/ad531e

What follows is a list of articles you may be interested in

Effect of Y element on atomic structure, glass forming ability, and magnetic properties of FeBC alloy

Jin-Hua Xiao(肖晋桦), Da-Wei Ding(丁大伟), Lin Li(李琳), Yi-Tao Sun(孙奕韬), Mao-Zhi Li(李茂枝), and Wei-Hua Wang(汪卫华)
Chin. Phys. B, 2024, 33 (**7**): 076101. DOI: 10.1088/1674-1056/ad3dd4

First-principles study of structural and opto-electronic characteristics of ultra-thin amorphous carbon films

Xiao-Yan Liu(刘晓艳), Lei Wang(王磊), and Yi Tong(童祎)
Chin. Phys. B, 2022, 31 (**1**): 016102. DOI: 10.1088/1674-1056/ac0cd8

Metabasin dynamics of supercooled polymer melt

Jian Li(李健), Bo-Kai Zhang(张博凯)
Chin. Phys. B, 2019, 28 (**12**): 126101. DOI: 10.1088/1674-1056/ab4e82

Versatile $GaInO_3$-sheet with strain-tunable electronic structure, excellent mechanical flexibility, and an ideal gap for photovoltaics

Hui Du(杜慧), Shijie Liu(刘世杰), Guoling Li(李国岭), Liben Li(李立本), Xueshen Liu(刘学深), Bingbing Liu(刘冰冰)
Chin. Phys. B, 2019, 28 (**1**): 016105. DOI: 10.1088/1674-1056/28/1/016105

Static and dynamic properties of polymer brush with topological ring structures: Molecular dynamic simulation

Wu-Bing Wan(万吴兵), Hong-Hong Lv(吕红红), Holger Merlitz(候格), Chen-Xu Wu(吴晨旭)
Chin. Phys. B, 2016, 25 (**10**): 106101. DOI: 10.1088/1674-1056/25/10/106101

Effect of interlayer bonded bilayer graphene on friction

Yao-Long Li(李耀隆)[1,2], Zhen-Guo Tian(田振国)[1,2], Hai-Feng Yin(尹海峰)[1,2], and Ren-Liang Zhang(张任良)[1,2,†]

[1] *Hebei Key Laboratory of Mechanical Reliability for Heavy Equipment and Large Structures, Yanshan University, Qinhuangdao* 066004, *China*

[2] *School of Civil Engineering and Mechanics, Yanshan University, Qinhuangdao* 066004, *China*

(Received 11 March 2024; revised manuscript received 9 May 2024; accepted manuscript online 3 June 2024)

We study the friction properties of interlayer bonded bilayer graphene by simulating the movement of a slider on the surface of bilayer graphene using molecular dynamics. The results show that the presence of the interlayer covalent bonds due to the local sp^3 hybridization of carbon atoms in the bilayer graphene seriously reduces the frictional coefficient of the bilayer graphene surface to 30%, depending on the coverage of interlayer sp^3 bonds and normal loads. For a certain coverage of interlayer sp^3 bonds, when the normal load of the slider reaches a certain value, the surface of this interlayer bonded bilayer graphene will lose the friction reduction effect on the slider. Our findings provide guidance for the regulation and manipulation of the frictional properties of bilayer graphene surfaces through interlayer covalent bonds, which may be useful for applications of friction related graphene based nanodevices.

Keywords: nanoscale friction, molecular dynamic simulation, bilayer graphene, interlayer covalent bond

PACS: 61.48.Gh, 62.20.Qp,31.15.xv **DOI:** 10.1088/1674-1056/ad531e

1. Introduction

Friction is a mechanical phenomenon that hinders the relative motion of two objects when their surfaces are in contact with each other and have a relative motion or relative motion trend.[1,2] The force that hinders their relative motion or relative motion trend is called frictional force. The essence of friction is the irreversible energy dissipation between two contact surfaces and the thermodynamic process involving complex non-equilibrium states.[3] According to statistics, about one-third of energy consumption is used to overcome friction in industrial production.[4] The phenomenon of friction is inevitable, but exploring the regulation and reduction of the impact of friction in the system has always been the direction of scientists' efforts. Under macroscopic conditions, for the friction between solids, it is generally believed that the rougher of the surface, the greater the frictional force under the same normal load conditions. Analyzing friction from the atomic level of the constituent materials, due to the discrete characteristics of the atomic structure, the smooth contact between the contact surfaces will become many rough peak contacts, so the macro friction theory will no longer be suitable for micro friction.

Graphene, a two-dimensional material with atomic thickness, is composed of carbon atoms with sp^2 hybridization and a hexagonal honeycomb structure. Due to its high chemical inertness, extreme mechanical strength, large specific surface area structure,[5] easy shear ability,[6] excellent lubrication performance,[7] and surface protection effect.[8] It has broad application prospects in the field of lubrication and nanomachine. For example, Verhoeven *et al.*[9] and Liu *et al.*[10] observed that graphite system exhibits super lubricity through theoretical and experimental methods. Based on super lubricating properties of graphene, Popov *et al.*[11] reported the self-retracting motion of a graphene flake on a stack of graphene flakes. Based on the self-retracting motion of a graphene flake, Jeong *et al.* proposed graphene nanoflakes devices moving on graphite ribbon controlled by electrostatic force and retraction van der Waals force,[12] designed nanoscale inertial sensor,[13] and nonvolatile graphene nanoflake shuttle memory.[14]

With the rapid development of industry, the pristine graphene has been unable to meet its needs, so the functionalized graphene has attracted more and more attention.[15] Functionalize graphene can alter various properties of graphene. For example, precise modulation of graphene local hybridization is used to open graphene bandgap.[16] Hydrogen fossil graphene is used for desalination of seawater.[17] Under static high pressure, multilayer graphene undergoes a direct phase transition from diamond, and a new type of hybrid carbon material with unique combinations of mechanical and electrical properties has been discovered.[18] Functionalization will also have a major influence on the friction properties of graphene. Ko and Kown *et al.* revealed hydrogenation, oxidation, and fluorination increase the surface friction of graphene by 2–7 times compared to ordinary graphene.[19,20] They attributed the increase in friction to the increase in bending phonon dissipation due to the greater out-of-plane bending stiffness. Fessler *et al.*[21] compared the friction silicon dioxide supported hydrogen graphene and original graphene through atomic force microscope. He believed that the greater friction on the surface of hydrogen graphene

†Corresponding author. E-mail: zhrleo@ysu.edu.cn

© 2024 Chinese Physical Society and IOP Publishing Ltd

was caused by its adsorption of more pollutants. Dong *et al.*[22] revealed that the surface of hydrogenated graphene has higher friction in molecular dynamics simulation, which is mainly due to the greater roughness of the surface of hydrogenated graphene. Li *et al.*[23] pointed out that the friction force of fluorinated graphene was greater than that of ordinary graphene due to the enhanced interaction between the interfaces caused by the introduction of fluorine atoms. Carbon atoms in multilayer graphene can be coupled between layers to form sp^3 bonds through methods such as high temperature annealing,[24] high pressure,[25] electron irradiation,[26] femtosecond laser,[27] and chemical reactions,[28] thereby altering the thermal[29–31] and mechanical properties[32] of interlayer bonded graphene or carbon nanotubes, sparking research interest in the impact of sp^3 hybridization between bilayer graphene layers on their performance.

In this paper, the molecular dynamics method is used to simulate the sliding process of graphene slider on the interlayer bonded graphene surface, to study the friction performance of the interlayer bonded graphene. The focus was on analyzing the influence of patterned distribution of interlayer sp^3 bonds, with coverage rate ranging from 0 to 12.5%, on the frictional force of graphene slider under different normal loads. At the same time, a detailed analysis was conducted on the influence of interlayer sp^3 bonded graphene surface on the distribution of frictional force in various regions of the slider. The research results supplement the relevant theory of friction on the surface of two-dimensional materials such as multilayer graphene with commensurate or incommensurate contact, help us to understand the interlayer sp^3 bonded graphene surface properties, which is essential for the fabrication of graphene-based electronic transistors,[33] and provide new ideas for surface motion control of nanodevices based on graphene.

2. Computational methods

In order to simulate the method of atomic force microscope testing surface friction, in this study we establish the system shown in Fig. 1. There are four layers of graphene in the simulate model, the top layer graphene is a slider used as a probe to simulate atomic force microscope, the size of graphene slider is 2.95 nm × 5.11 nm, containing 600 carbon atoms in total. The middle two layers of graphene are the detected materials, the size of each layer of graphene is 20.16 nm × 5.11 nm, contains 3936 atoms. The middle part of these bilayer graphene locally forms interlayer sp^3 bonds, the coverage of interlayer sp^3 bonds is defined as the ratio of the number of carbon atoms bonded to the total number of carbon atoms in a layer, which is the same as the literature.[34] The bottom layer is a spring supported substrate, which is similar to the work of Chang *et al.*,[35] and the support stiffness of the spring is adjusted to simulate the support of different material surfaces. Based on theoretical calculation of the spring stiffness between two adjacent graphene layers,[35,36] a spring constant k_s of 2.7 N/m is used in this study.

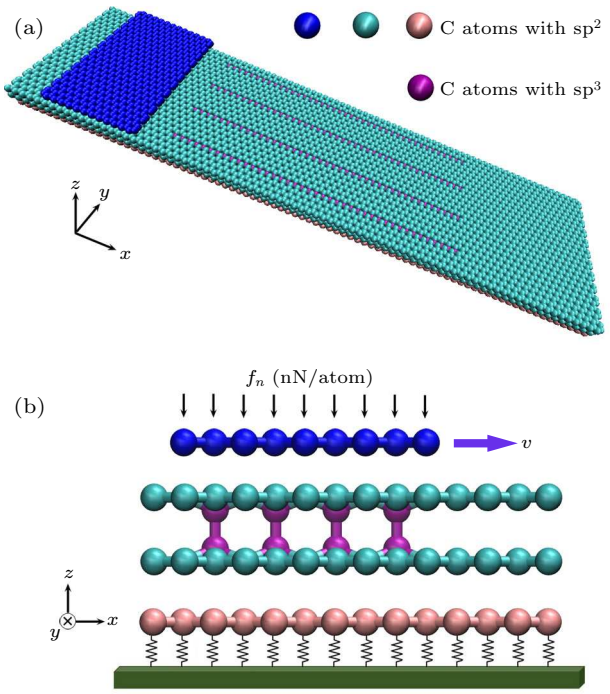


Fig. 1. Configurations of the simulation system. (a) A graphene slider is placed on a rectangular interlayer bonded bilayer graphene substrate. (b) Each carbon atom within the graphene supporting is connected to a linear spring $k_s = 2.7$ m/s along the z-direction. A normal load f_n is applied to each atom of the slider, and the slider slides against the interlayer bonded bilayer graphene substrate along the x-direction with the velocity of $v = 10$ m/s. In the snapshot, the sp^2 hybridized carbon atoms are represented by the blue, the cyan and the pink color, and the sp^3 hybridized carbon atoms are represented by the purple color.

The simulation is performed by using the molecular dynamics method with a large-scale atomic molecular massively parallel simulator. The adaptive intermolecular reactive empirical bond order Airebo potential is used to describe the intralayer carbon–carbon bond interaction, and the interlayer interaction is described by Lenard–Jones potential (with a well depth of $\varepsilon = 2.968$ meV and an equilibrium $\sigma_{OC} = 3.407$ Å), as they were in previous studies.[35,37,38] For the slider, fix its rotation along z-direction, and it is pulled along the x-direction through a spring. For the bilayer graphene and spring supported substrate, the center of mass is fixed along the x- and y-directions. Periodic boundary conditions are applied to the substrate along the y-directions, while free boundary condition is imposed along the x-direction and z-direction. The entire simulation process was conducted under the NVT ensemble, and the temperature of the simulation system was controlled at 300 K using the Nose–Hoover temperature control method, with a simulation time step of 0.0005 ps.

The simulation process is divided into three steps. Firstly, a relaxation of 100 ps is performed to bring the system to an equilibrium state. Apply a normal load f_n to each atom of

the slider, and then perform a 100 ps relaxation to restore the system to equilibrium. Then the simulation of sliding friction is started. The center of mass of the slider is connected to a virtual ball that moves at a constant speed of 10 m/s along the x-direction through a linear spring with a stiffness of $K_t = 36$ N/m. The virtual ball pulls the slider to stick and slide along the x-direction through the spring. The frictional force on the slider is the average of component of the interaction force between the layers of bilayer graphene and the slider over 1.5 ns along the sliding direction. The frictional coefficient is defined as the ratio of the normal force to the tangential force on the slider.

3. Results and discussion

3.1. Effect of interlayer covalent bonds

We used the molecular dynamics method to simulate the motion of the slider on the surface of graphene, and calculated the frictional force and frictional coefficient of the surface of pristine bilayer graphene and bilayer graphene with a certain coverage of interlayer sp^3 bonds under a load of 0.05 nN/atom. For the convenience of comparison, under the same coverage of interlayer sp^3 bonds, both random distribution and pattern distribution are considered separately, the results are shown in Fig. 2.

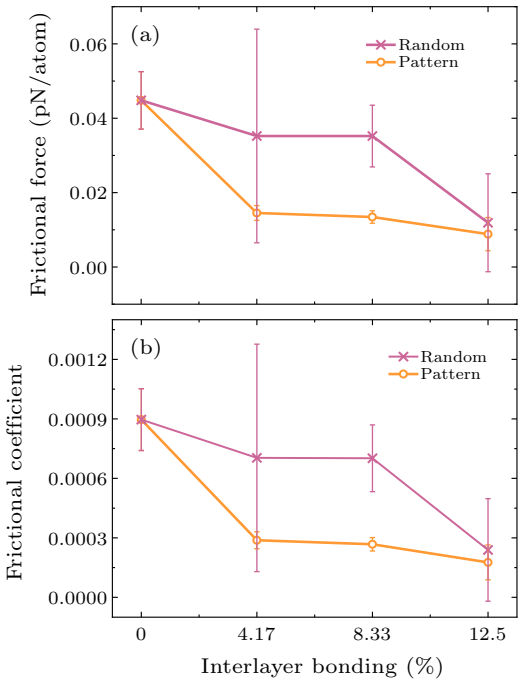


Fig. 2. Schematic of a bilayer graphene with interlayer bonding to the frictional force (a) and frictional coefficient (b).

The results show that the presence of interlayer sp^3 bonds greatly affects the friction performance of the bilayer surface. Under the same normal load, the surface of bilayer graphene with interlayer sp^3 bonds has less friction than the pristine bilayer graphene. The frictional coefficient of the interlayer bonded bilayer graphene decreases with the increase of coverage of interlayer sp^3 bonds, at 12.5% coverage of interlayer sp^3 bonds, the bilayer graphene surface with interlayer sp^3 bonds reaches a superlubricity state.[39] From the perspective of reducing the stability of frictional coefficient, it can be seen that compared to random distribution, pattern distribution appears more stable, mainly due to the randomness of random distribution. Therefore, we will mainly analyze pattern distribution next.

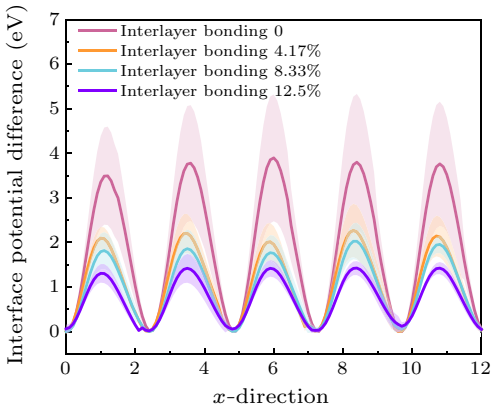


Fig. 3. Variation of interface potential difference between the slider and the substrate with different sp^3 probability patterned distributions in the x-direction.

In order to further investigate the mechanism of pattern distribution reducing frictional coefficient, it is helpful to analyze the potential energy between the slider and bilayer graphene substrate. Therefore, the interface potential difference between the slider and bilayer graphene substrate is calculated, where the interface potential difference is defined as the difference between the potential energy and minimum potential energy values, so the difference between the maximum and minimum potential energy is interfacial potential barrier. We calculate the interface potential difference along the x-direction for both the pristine bilayer graphene and bilayer graphene with different coverage of interlayer sp^3 bonds, as shown in Fig. 3. The results show that the interface potential difference of both the pristine graphene surface and the interlayer bonded bilayer graphene surface vary with the x position and exhibit periodic characteristics, which is consistent with the lattice size of graphene. The results also show that the pristine bilayer graphene has the largest interface potential barrier, with a maximum value of approximately 3.9 eV. The interlayer bonded bilayer graphene has lower interface potential barrier than the pristine bilayer, and the maximum value of interface potential barrier decreases with the increase of coverage rate of sp^3 hybrid. When the coverage of interlayer sp^3 bonds reaches 12.5%, the interface potential barrier is only 1.5 eV. This means that sliding the slider on an interlayer bonded bilayer graphene surface requires less energy than sliding on pristine bilayer graphene surface, and as the

coverage of interlayer covalent bonds increases, sliding becomes easier and the frictional force is smaller, as shown in Fig. 2.

The slider moves on a substrate, and when there is a normal load, any non rigid substrate will undergo out-of-plane deformation, which affects the friction of the slider.[40–42] To investigate the reasons for the decrease in frictional force caused by bilayer graphene substrates with covalent bonds, we calculated the normal deformation energy of pristine bilayer graphene and interlayer-bonds bilayer graphene substrates with different coverage of interlayer sp^3 bonds when the normal load is 0.05 nF/atom.

We first apply different normal loads to the slider, then calculate the indentation depth δ of the pristine bilayer graphene substrate and interlayer bonded bilayer graphene in contact with the slider, and obtain the stiffness K of the pristine bilayer graphene substrate and the interlayer bonded bilayer graphene substrate with different coverages of interlayer sp^3 bonds by calculating their slope, as shown in Fig. 4(a). According to Ref. [42] we calculate the deformation energy ($E = \frac{1}{2}K\delta^2$) of the bilayer substrate, the out-of-plane deformation energy of the substrate under a normal load of 0.05 nF/atom is shown in Fig. 4(b).

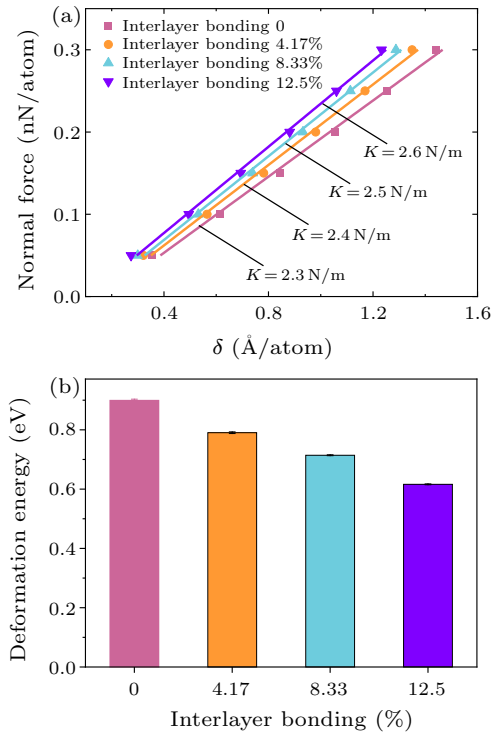


Fig. 4. Calculation of normal deformation of the bilayer graphene substrate with different coverages of interlayer sp^3 bonds. (a) The relationship between normal load and indentation depth. (b) Normal deformation energy of substrates with different interlayer sp^3 bonds under a normal load of 0.05 nF/atom.

Figure 4(a) shows the indentation depth of the substrates in contact with the slider under different normal loads. We can see that under the same normal load, the pristine bilayer graphene substrate has the maximum indentation depth, and the indentation depth of the interlayer bonded bilayer graphene substrate decreases with the increase of interlayer sp^3 bonds. It shows that the interlayer sp^3 bonds between the bilayer graphene substrate will lead to the increase of its out-of-plane bending stiffness, and its out-of-plane bending stiffness increases with the increase of interlayer sp^3 bonds. Although the stiffness of interlayer bonded bilayer graphene substrate increases, the out-of-plane deformation energy of the interlayer bonded bilayer graphene substrate is relatively low because the indentation depth is lower than that of the pristine bilayer graphene, and under the same load conditions, the normal deformation energy decreases with the increase of the coverage of interlayer sp^3 bonds, as shown in Fig. 4(b).

When a slider under a normal load slides on the substrate, in addition to overcoming the interface potential barriers of the substrate, it also needs to overcome the normal deformation energy of the substrate. The greater the normal deformation energy of the substrate, the greater the frictional force that the slider will experience.

As described above, compared with the pristine bilayer graphene, the interlayer bonded bilayer graphene has smaller interface potential barriers and smaller out-of-plane deformation energy, which is the reason for reduction of the slider friction, and the frictional coefficient on its surface can be regulated through the coverage of interlayer sp^3 bonds.

3.2. Effect of normal load

It is found that when the normal load increases to a certain extent, the superlubricity of material will be failure.[43–46] Inspired by this viewpoint, this article next investigates the effect of normal loads. Here, when the slider slides on the bilayer graphene surface, we change the normal load of the slider and calculate the frictional force of the slider on the bilayer graphene surface with different coverage of interlayer sp^3 bonds, as shown in Fig. 5.

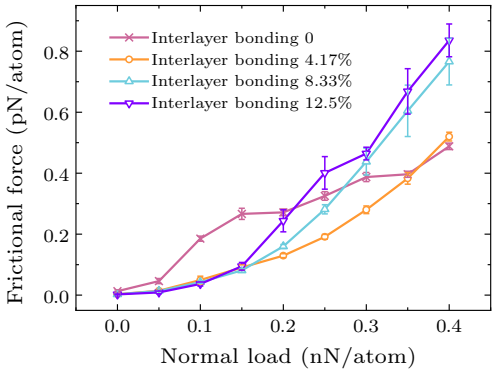


Fig. 5. Effect of normal load on the frictional force of slider sliding on the bilayer graphene surfaces with different coverages of interlayer sp^3 bonds.

Figure 5 shows the frictional force of the slider on the bilayer graphene surface with different coverages of interlayer sp^3 bonds under different normal load of the slider. It can

be seen from Fig. 5 that the frictional force of the slider increases with the normal load whether it is the pristine bilayer graphene substrate or interlayer bonded bilayer graphene substrate. For the pristine bilayer graphene substrate, the frictional force of the slider increases linearly with the normal load, but for the interlayer bonded bilayer graphene substrate, the frictional force increases nonlinearly with the increase of the normal load, and the greater the normal load, the larger the frictional force. From Fig. 5 we also see that when the normal load is small, the frictional force of the slider on the interlayer bonded bilayer graphene substrate is smaller than that on the pristine bilayer graphene substrate, indicating that the interlayer bonded bilayer graphene substrate can reduce the resistance of the slider at this time, when the normal load is 0.15 nN/atom, the frictional force of the slider on an interlayer bonded bilayer graphene substrate is approximately 30% of the frictional force on the pristine graphene substrate. When the normal load increases, the frictional force of the slider on the interlayer bonded bilayer graphene substrate is higher than that on the pristine bilayer graphene substrate. As the coverage of interlayer sp^3 bonds increases, the frictional force of the slider increases, and the advantage of interlayer bonded bilayer substrate in reducing friction resistance gradually disappears, for example, when the normal load is 0.2 nN/atom, the frictional force of the slider on the interlayer bonded bilayer graphene substrate with 12.5% coverage of interlayer sp^3 bonds is higher than that on the pristine graphene substrate. When the load is 0.3 nN/atom, the frictional force of the slider on the interlayer bonded bilayer graphene substrate with 8.33% coverage of interlayer sp^3 bonds is higher than that on the pristine graphene substrate. When the load is 0.4 nN/tom, the frictional force of the slider on the interlayer bonded bilayer graphene substrate with 4.17% coverage of interlayer sp^3 bonds is higher than that on the pristine graphene substrate.

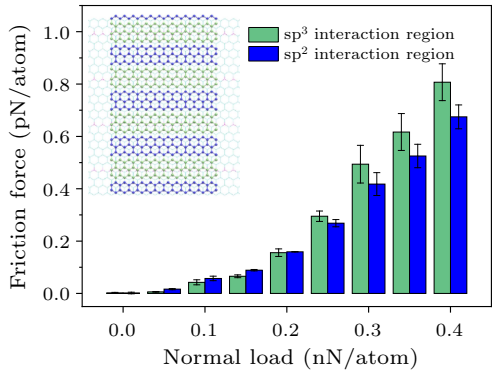


Fig. 6. Variation of average frictional force on atoms of slider interacting with sp^3 hybridized atoms and sp^2 hybridized atoms in the substrate with 8.33% coverage of interlayer sp^3 bonds under different normal load.

In order to further study the influence of local sp^3 hybridized atoms in the substrate on the frictional force of the slider, we take the interlayer bonded bilayer graphene substrate with 8.33% coverage of interlayer sp^3 bonds as an example, and divided the slider evenly into two regions with 300 atoms per region as shown in Fig. 6, that is, the region that mainly interacts with sp^3 hybridized atoms in the substrate and the region that mainly interacts with sp^2 hybridized atoms in the substrate. According to this division method, the average frictional force of each atom in these two regions of the slider under different normal loads was calculated, as shown in Fig. 6.

Figure 6 shows the average frictional force of atoms in the slider interacting with the sp^3 and sp^2 hybrid regions of the substrate as a function of normal load. It can be seen that the average frictional force of atoms in these two regions increases nonlinearly with the increase of normal load. When the normal load is small, the average frictional force of the atoms in the slider interacting with the sp^3 hybridized atoms in the substrate is smaller than that of the atoms interacting with the sp^2 hybridized atoms in the substrate. However, when the normal load is large, the average frictional force of the atoms in the slider interacting with the sp^3 hybridized atoms in the substrate is greater than that of the atoms interacting with the sp^2 hybridized atoms in the substrate.

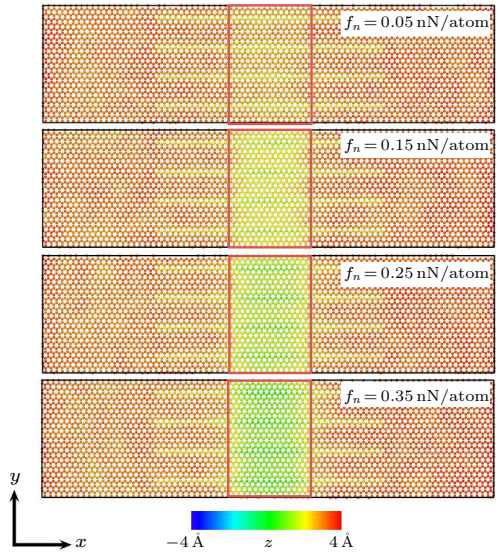


Fig. 7. Structural evolution diagram of interlayer bonded bilayer graphene substrate under different normal loads (the red border area represents the position of the slider).

According to reports,[1,18,47] the mechanical properties and microstructure of graphene change with the presence of ripples induced by the hybridization of carbon atoms from sp^2 to sp^3. In this simulation, the same phenomenon has also been observed. When bilayer graphene local atoms sp^3 hybridize, covalent bonds are formed between layers. The associated changes in the geometry brought about by these sp^3 hybridized atoms are that these atoms are moved away from the planar graphene, and the local structure is no longer planar and forms ripples, as shown in Fig. 7. For non-rigid substrates, when the slider is subjected to a normal load, the substrate has

an out-of-plane deformation. The out-of-plane deformation of the substrate in the area of interaction with the slider is significant and increases with the increase of the normal load on the slider. When the normal load is small, the out-of-plane deformation of the substrate is small, the ripples induced by the hybridization of carbon atoms from sp^2 to sp^3 still exist as shown in the top of Fig. 7, which makes the contact between the slider and the substrate evolve from commensurate to incommensurate contact, leading to the decrease of friction force. This is consistent with previous reports[48] on the main role of interface commensurability in interlayer friction. When the normal load increases, the out-of-plane deformation of the substrate in the area of interaction with the slider is significantly different from that of the non-interaction area. In the area of non-interacting with the slider, the ripples caused by the hybridization of carbon atoms from sp^2 to sp^3 still exist, and in the area of interacting with the slider, the heights of sp^2 and sp^3 atoms tend to be consistent as shown in the bottom of Fig. 7. This structural change means that a large energy is required to slide the flake against the bonded bilayer graphene surface, resulting in greater friction of the atoms interacting with the substrate sp^3 hybrid region in the slider than that of the atoms interacting with the substrate sp^2 hybrid region, which is consistent with Fig. 6. Therefore, the local sp^3 hybrid atoms on the substrate cause structural changes, resulting in nonlinear changes in the frictional force on sliding with increasing normal load. When the normal load is small, the interlayer bonds bilayer graphene substrate has a friction reduction effect, and when the normal load increases, it has a friction increment effect, which is consistent with Fig. 5.

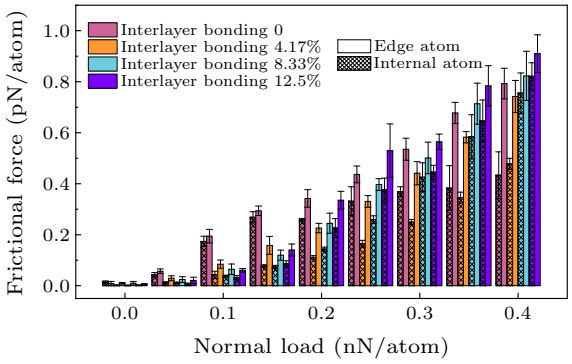


Fig. 8. Variation of the average frictional force on the edge and internal atoms of the slider with normal load.

In order to conduct a more in-depth analysis of the frictional forces acting on the atoms that make up the slider, we calculated the spatial distribution of frictional forces on the slider. We first divided the atoms of the slider into edge atoms (at each end of the boundary perpendicular to the direction of motion of the slider) and internal atoms (between the boundaries at both ends). Then, calculated the average frictional force acting on these two parts of the atoms, as shown in Fig. 8.

It can be seen from Fig. 8 that no matter whether it is a pristine bilayer graphene substrate or interlayer bonded graphene substrate, with the increase of the normal load of the slider, the average frictional force between the edge atoms and the internal atoms of the slider increases simultaneously. For pristine bilayer graphene substrate, the average frictional force of the edge atoms and internal atoms of the slider increases linearly with the increase of the normal load of the slider, which is consistent with the results reported in the literature.[49] However, for interlayer bonded bilayer graphene substrate, as the normal load of the slider increases, the average frictional force of edge atoms and internal atoms of the slider exhibit nonlinear relationships, respectively. When the normal load is small, the average frictional force of the edge atoms and the internal atoms of the slider on the interlayer bonded bilayer graphene substrate is smaller than that on the pristine bilayer graphene substrate. However, when the normal load is large, it is quite the reverse. Meanwhile, from Fig. 8, we can also see that under the same normal load, the average frictional force of the edge atoms and the internal atoms of the slider on the interlayer bonded bilayer graphene substrate increase with the increase of the coverage of interlayer sp^3 bonds, respectively. The interlayer bonded bilayer graphene substrate will bring complex boundary effects to the slider, which is different from the pristine bilayer graphene substrate.

4. Conclusions

We have systematically studied the effect of interlayer covalent bonds on the friction properties of bilayer graphene by molecular dynamics method. It is found that the frictional properties of the interlayer bonded graphene surfaces strongly depend on the coverage of interlayer sp^3 bonds and normal loads. For interlayer bonded bilayer graphene, the frictional coefficient gradually decreases with the increase of the coverage of interlayer sp^3 bonds due to reduction of interface potential barrier and normal deformation energy under small normal loads. On the contrary, under large normal loads, the larger the coverage of the interlayer sp^3 bonds is, the greater the frictional coefficient of the interlayer bonded bilayer graphene is. The presence of interlayer sp^3 bonds seriously affects the spatial distribution of frictional force during sliding of the slider on the interlayer bonded bilayer graphene. These findings may have an important role in motion regulation applications of graphene based nanodevices.

Acknowledgments

The project supported by the Doctor Fund and the Program of independent Research for Young Teachers of Yanshan University (Grant Nos. B919 and 020000534). The authors also thank the High Performance Computing and Data Center,

School of Civil Engineering and Mechanics, Yanshan University.

References

[1] Peng Y, Li J, Tang X, Liu B, Chen X and Bai L 2020 *Tribol. Lett.* **68** 22
[2] Hanaor D A, Gan Y and Einav I 2016 *Tribol. Int.* **93** 229
[3] Li Y, Li S, Wang M and Zhang R 2024 *Chin. Phys. B* **33** 046101
[4] Holmberg K and Erdemir A 2017 *Friction* **5** 263
[5] Novoselov K S, Fal'ko V I, Colombo L, Gellert P R, Schwab M G and Kim K 2012 *Nature* **490** 192
[6] Berman D, Erdemir A and Sumant A V 2014 *Mater. Today* **17** 31
[7] Sun J and Du S 2019 *RSC Adv.* **9** 40642
[8] Berman D, Erdemir A and Sumant A V 2014 *Appl. Phys. Lett.* **105** 231907
[9] Verhoeven G S, Dienwiebel M and Frenken J W 2004 *Phys. Rev. B* **70** 165418
[10] Liu Z, Yang J, Grey F, Liu J Z, Liu Y, Wang Y, Yang Y, Cheng Y and Zheng Q 2012 *Phys. Rev. Lett.* **108** 205503
[11] Popov A M, Lebedeva I V, Knizhnik A A, Lozovik Y E and Potapkin B V 2011 *Phys. Rev. B* **84** 245437
[12] Kang J W, Park J and Kwon O K 2014 *Physica E* **58** 88
[13] Kim S Y, Cho S Y, Kim K S and Kang J W 2013 *Physica E* **50** 44
[14] Hwang H J and Kang J W 2014 *Physica E* **56** 17
[15] Jeong J H, Kang S, Kim N, Joshi R and Lee G H 2022 *Phys. Chem. Chem. Phys.* **24** 10684
[16] Yu M, Chen C, Liu Q, Mattioli C, Sang H, Shi G, Huang W, Shen K, Li Z and Ding P 2020 *Nat. Chem.* **12** 1035
[17] Chogani A, Moosavi A, Bagheri Sarvestani A and Shariat M 2020 *J. Mol. Liq.* **301** 112478
[18] Li Z, Wang Y, Ma M, Ma H, Hu W, Zhang X, Zhuge Z, Zhang S, Luo K, Gao Y, Sun L, Soldatov A V, Wu Y, Liu B, Li B, Ying P, Zhang Y, Xu B, He J, Yu D, Liu Z, Zhao Z, Yue Y, Tian Y and Li X 2023 *Nat. Mater.* **22** 42
[19] Ko J H, Kwon S, Byun I S, Choi J S, Park B H, Kim Y H and Park J Y 2013 *Tribol. Lett.* **50** 137
[20] Kwon S, Ko J H, Jeon K J, Kim Y H and Park J Y 2012 *Nano Lett.* **12** 6043
[21] Fessler G, Eren B, Gysin U, Glatzel T and Meyer E 2014 *Appl. Phys. Lett.* **104** 041910
[22] Dong Y, Wu X and Martini A 2013 *Nanotechnology* **24** 375701
[23] Li Q, Liu X Z, Kim S P, Shenoy V B, Sheehan P E, Robinson J T and Carpick R W 2014 *Nano Lett.* **14** 5212
[24] Tang C, Zhang Y, Guo W and Chen C 2010 *J. Phys. Chem. C* **114** 18091
[25] Martins L G P, Matos M J, Paschoal A R, Freire P T, Andrade N F, Aguiar A L, Kong J, Neves B R, de Oliveira A B and Mazzoni M S 2017 *Nat. Commun.* **8** 96
[26] Peng B, Locascio M, Zapol P, Li S, Mielke S L, Schatz G C and Espinosa H D 2008 *Nat. Nanotechnol.* **3** 626
[27] Kanasaki J, Inami E, Tanimura K, Ohnishi H and Nasu K 2009 *Phys. Rev. Lett.* **102** 087402
[28] Kvashnin A G, Chernozatonskii L A, Yakobson B I and Sorokin P B 2014 *Nano Lett.* **14** 676
[29] Tang C, Zhang Y, Guo W and Chen C 2010 *J. Phys. Chem. C* **114** 18091
[30] Chien S K, Yang Y T and Chen C K 2011 *Appl. Phys. Lett.* **98** 033107
[31] Li Y, Li Z, Li S and Zhang R 2023 *Acta Phys. Sin.* **72** 243101 (in Chinese)
[32] Xia Z, Guduru P and Curtin W 2007 *Phys. Rev. Lett.* **98** 245501
[33] Albarakaty H A 2016 US Patents No. 9 318 348 B2 [2016-04-19]
[34] Guo T, Sha Z D, Liu X, Zhang G, Guo T, Pei Q X and Zhang Y W 2015 *Appl. Phys. A* **120** 1275
[35] Chang T, Zhang H, Guo Z, Guo X and Gao H 2015 *Phys. Rev. Lett.* **114** 015504
[36] Wang K, Qu C, Wang J, Ouyang W, Ma M and Zheng Q 2019 *ACS Appl. Mater. Interfaces* **11** 36169
[37] Chen J, Gao Y, Wang C, Zhang R, Zhao H and Fang H 2015 *J. Phys. Chem. C* **119** 17362
[38] Zhang R, Li S, Li Y and Wang M 2022 *J. Nano Res.* **74** 97
[39] Wang K, Ouyang W, Cao W, Ma M and Zheng Q 2019 *Nanoscale* **11** 2186
[40] Kim H J and Chung K H 2020 *Appl. Surf. Sci.* **534** 147629
[41] Yitian, Peng, Xingzhong, Zeng, Lei, Liu, Xingan, Cao, Kun and Zou 2017 *Carbon* **124** 541
[42] Smolyanitsky A, Killgore J P and Tewary V K 2012 *Phys. Rev. B* **85** 035412
[43] Chen X and Li J 2020 *Carbon* **158** 1
[44] Li J, Li J and Luo J 2018 *Adv. Sci.* **5** 1800810
[45] Kim W K and Falk M L 2009 *Phys. Rev. B* **80** 235428
[46] Van Wijk M, Dienwiebel M, Frenken J and Fasolino A 2013 *Phys. Rev. B* **88** 235423
[47] Sofo J O, Chaudhari A S and Barber G D 2007 *Phys. Rev. B* **75** 153401
[48] Hod O, Meyer E, Zheng Q and Urbakh M 2018 *Nature* **563** 485
[49] Zhang H and Chang T 2018 *Nanoscale* **10** 2447